

## ALTERNATIVE METHOD TO INITIALIZE REGIONAL OCEAN MODELS USING GEOSTROPGIC VELOCITIES: APPLICATION TO THE BAY OF BISCAY

J. Nogueira • H. Coelho • M. Juliano • P. C. Leitão

### CHAPTER SYNOPSIS

#### Background

An alternative initialization method to [1] was developed to reduce the spin up time on regional Ocean Model simulations. The method was applied to the regional model of the circulation in the Bay of Biscay. Two initialization schemes were tested and compared using *in situ* data (Argo floats and microwave SST); a *slow start* initialization where the model starts at rest and forces were slowly switched [1]; a direct initialization where the model starts with initial velocity, sea level fields and forces switched on.

#### Results

Both gives a final circulation pattern compatible with the literature but the results shown that the direct initialization with a geostrophic velocity field computed from sea level and density fields of the global model leads to an improved thermohaline structure in the deep layers of the ocean.

#### Conclusions

The low computational cost and the quality of the results justify the application this method in operational schemes.

## 1 INTRODUCTION

Numerical Ocean models are based on the resolution of Navier-Stokes equations for a specific physical situation. Like all differential equations, they admit an infinite number of solutions and just one represents our physical problem. The determination of this solution is made by the choice of the boundary conditions and further, the choice of the initial condition. Even with a good choice of boundary conditions, an unbalanced initial condition can leads the numerical model to unrealistic motions during the initialization transient process (mostly inertial-gravity waves) with the consequence of an irreversible state far from the true one. Transient processes generated with a crude initialization have important consequences on the long-term model trajectory [2]. The rigid-lid approximation on large-scale ocean models can filter out those quickly propagating inertia-gravity waves [3]. For free-surface models this is not true and a careful spin up must be done to avoid undesirable consequences like the destruction of the initial state or divergence of the model [4]. Several techniques based on a nudging method were tested to filter out this noise [5-6]. The price paid by these techniques is a loss of physical realism during the spin up period.

In coastal models, Open Boundary Conditions (OBC) can also be important to prevent undesirable consequences caused by the inertial-gravity waves generated during the initialization process. In fact Radiation Boundary conditions can prevent reflections of such waves. A set of Boundary Conditions [7] can be constructed, in which a Flow Relaxation Scheme (FRS) applied to temperature (T), salinity (S) and velocities (U, V) [8] is combined with a radiation scheme [9] for the barotropic mode. This boundary condition scheme was used in MOHID by [10]. However, initial state is still a problem that must be carefully treated and as previously shown, a full set of initial and boundary conditions must be estimated [11].

Different approaches were developed to define an optimal state that makes the initial field (observations) physically consistent with a model. A complete review of those methods was made by [12]. [4] developed a strong methodology to construct a consistent initial state based on optimal interpolation applied to an inverse method. This method ensures that the initial state satisfies the fundamental mass balance, avoiding the generation of mass fluxes associated with a crude interpolation/extrapolation scheme. An application of this method to the Gulf of Lion where a compromise between computational cost and equilibrium of initial state was considered reproduced the main hydrological and circulation patterns [13].

When a combined scheme of open boundary conditions with radiation and flow relaxation is used on a regional ocean model, a reference solution must be given. Usually this reference solution is obtained with climatological fields, from a set of data, or from a global ocean model with lower resolution. For downscaling methodology, where the reference solution is given by a global ocean model, the initialization and forcing of the embedded model can be done with a variational initialization and forcing platform (VIFOP) where the variational strategy ensure that the forcing fields satisfy the fundamental mass balance [14]. This methodology was applied in the framework of the international project MFSTEP [15].

The problem of the regional model initialization in a downscaling approach can also be done with a scheme where the global solution is interpolated/extrapolated to the regional model grid and the forcing terms are slowly switched [1]. This methodology can prevent large gradients that may result from inconsistencies between forcing mechanisms (wind and tide) and the initial density field. This methodology reduces the spin up period and gives a solution able to reproduce the main features of a regional model (see [1] for a detailed description of the methodology). For operational applications, this initialization has at least two problems: the spin up time is yet too large and smooths the density gradients.

In this paper our objective is to construct an initial state for a regional ocean model consistent with the reference solution for OBC. This state must have a low computational cost and further, it should be a good approximation to the dynamic state for the ocean given by the initial reference solution. The methodology used is very simple and consists on the construction of an initial model state based on the reference solution. An interpolation/extrapolation of the mass field (density and water level) from the reference solution into the model grid is processed. With the field obtained the correspondent geostrophic velocities are computed. This state, near the dynamic equilibrium and consistent with the global model, allows to switch directly the forcing terms. Since the global model does not have tidal forcing, the correspondent terms are slowly switched at the open boundaries. In a downscaling methodology, this method was successfully applied to a 3 level nesting model of the estuarine Tagus plume [16].

A two level one-way nesting model is implemented for which the level 1 is a 2D barotropic tidal-driven model with a variable horizontal resolution ( $0.03^\circ$ - $0.04^\circ$ ) covering all the Bay of Biscay. The level 2 is a 3D baroclinic model with the same horizontal resolution. Two runs of 1 year with different initialization methods are compared. For the comparative analysis the reference solution and a set of available data (Argo floats and Microwave SST images) have been used.

## 2 METHODOLOGY

### 2.1 The model

The MOHID system uses a finite volume approach [17-18] to discretize the primitive equations. In this approach, the discrete form of the governing equations is applied macroscopically to a control volume. This makes the actual way of solving the equations independent of cell geometry and permits the use of a generic vertical coordinate that allows minimizing the errors of some of the classical vertical coordinates [18]. The equations are discretized horizontally in an Arakawa-C manner staggered grid. The temporal discretization is carried out by means of a semi-implicit (ADI) algorithm with two time levels per iteration.

The domain is defined between (-10.58; -0.734) E and (43.3; 49.9) N. The bathymetry used for the intercomparison is from SHOM (Service Hydrographique et Oceanographique de la Marine) and presents an initial resolution of 1'. No measure was undertaken in the Spanish territorial waters, thus, the bathymetry there is taken from ETOPO.

A variable horizontal resolution ( $0.03^{\circ}$ - $0.04^{\circ}$ ) is used and the vertical discretization is the same used by Mercator (43 layers, with the following thicknesses from the surface to the bottom: 6.26; 7.01; 7.49; 8.65; 9.46; 11.02; 12.31; 14.43; 16.37; 19.27; 22.13; 26.09; 30.17; 35.52; 41.17; 48.26; 55.81; 64.93; 74.61; 85.88; 97.64; 110.86; 124.32; 138.89; 153.27; 168.26; 182.54; 196.9; 210.08; 222.94; 234.31; 245.15; 254.39; 263.09; 270.24; 276.96; 282.26; 287.3; 291.11; 294.83; 297.49; 300.21; 302.01).

### 2.2 OBC and Initialization

The solution from the Mercator-Océan PSY2V1 system for the 2004 period was interpolated for the new grid with triangulation in the horizontal and with linear interpolation in the vertical. For the extrapolation procedure, the nearest neighbour approach was used (straight-forward method of assuming null horizontal gradient). The atmospheric fields (momentum and heat fluxes at the surface boundary) used to force the model are provided by the Météo-France of a high resolution (spatial  $0.1^{\circ}$  and 3 hour time step) forecast system - Aladin. For this study, only the three main French rivers were considered: Loire, Gironde and Adour. The Loire and the Gironde flows are greater than the Adour flow, by at least a ten-fold factor.

One of the main conclusions that come out from [7] is that to impose a consistent open boundary condition it is necessary to have a good reference solution (in this case the Mercator solution). In this work, to define the open boundary condition, a similar methodology to the one presented [10].

For the spin-up procedure two methodologies were tested. The first implemented is based on a slow connection of the forces - Slow Start [1]. This methodology consists in defining an initial condition where salinity and temperature initial fields are interpolated/extrapolated from the Mercator solution and null velocity field and sea level gradient are assumed. A coefficient that varies linearly between 0 and 1 along the "connection" period of 5 days is multiplied by the baroclinic force and wind stress. This method was applied for the Algarve coastal circulation [1] reproducing many of the features described in the literature.

In the second methodology used all forces (except tidal force) are switched on at the first iteration - direct initialization. The velocity and sea surface height initial fields have non zero values consistent with the salinity and temperature initial fields, through the geostrophic equilibrium (Figure 1). Tidal force is switch progressively in a linear way along of the first 12 hours.

### 2.3 Data

To compare and validate the results of the two initialization methods and of the Mercator solution, *in situ data* from Argo float<sup>1</sup> profiles and satellite sea surface temperature (SST) measurements from Advanced Microwave Scanning Radiometer<sup>2</sup> are used.

The Argo float [19] descends to a pre-programmed parking depth (typically 1000 to 2000 m) and drifts freely. Every 10 days it ascends from its parking depth to the sea surface. As it rises, temperature and salinity are measured continuously and transmitted to satellite when arrived at the surface. After the transmission, the float descends again and starts a new cycle. The global Argo profiles and trajectories are managed by the Global Ocean Data Assimilation Experiment and available from <http://www.usgodae.org>. We get all profiles fondly in the region during the period January 2004 to December 2004 and this where compared with the model's data results (resulting from the linear interpolation of the model data to the same location and time period of the Argo float profile). Only profiles with a quality flag indicating 'good data' and 'probably good data', have been used. The two resulting profiles (each model run and Argo floats) where then statistical compared and analyzed. Vertical profiles of temperature, salinity and density and T-S diagrams with model and Argo data, where also elaborated to analyse the thermohaline structure.

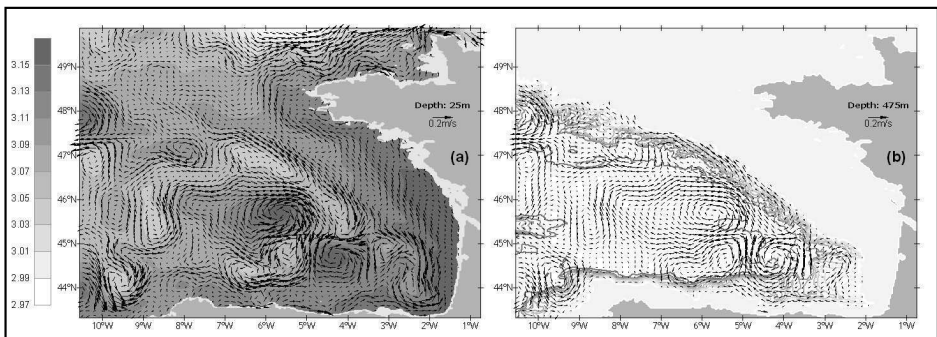


**Figure 1.** (a) Initial field of Sea Surface Height (grey scale) and Surface geostrophic velocities at 25 m deep. (b) Bathymetry (contour interval is 500 m) and Surface geostrophic velocities at 475 m deep.

<sup>1</sup>These data were collected and made freely available by the International Argo Project and the national programmes that contribute to it. (<http://www.argo.ucsd.edu>, <http://argo.jcommops.org>). Argo is a pilot programme of the Global Ocean Observing System.

<sup>2</sup>Microwave OI SST data are produced by Remote Sensing Systems and sponsored by National Oceanographic Partnership Program (NOPP), the NASA Earth Science Physical Oceanography Program, and the NASA REASON DISCOVER Project. Data are available at [www.remss.com](http://www.remss.com).

For the SST measurements we get a multi-sensor improved SST product derived from optimally Interpolated sea surface temperature (MISST) collected by Microwave Radiometer SSTs (AMSR-E, TMI). The data are available from <http://www.remss.com>. We have used daily MISST images, on a  $0.25^\circ$  longitude by  $0.25^\circ$  latitude grid, covering the Biscay Bay. They are different SST products resulting from a combination of satellite measurements and *in situ* observations (e.g., [20]). However, infrared measurements are strongly influenced by water vapour and cloud contamination [21], which can cause biases in regions where cloud cover is nearly constant. This means that studies using infrared SST data in those regions must often use composite images at weekly or monthly time intervals. In contrast to infrared radiation, microwave radiation is capable of penetrating through cloud. Also, the daily images actually distributed by the data servers, can be used in real time to validate the forecasting systems models, despite the lower horizontal resolution (when compared with high resolution infrared images). The daily MISST images have been statistical compared with the daily sea surface temperature from MOHID model data. For this purpose, the SST model data were daily averaged to the MISST resolution grid. An annual evolution of the resulting statistical parameters was also performed for both initializations methods and for the Mercator solution.

### 3 RESULTS AND DISCUSSION

#### 3.1 Energy Analysis

Figure 2 shows the kinetic energy and enstrophy behaviour of the model for the first month. Both initializations lead model to a stable solution in the first 7 days, but with the geostrophic velocities initialization the system goes faster to a state near to equilibrium. Further, Slow start initialization loses some kinetic energy as a result of the initial deviation from equilibrium.

The proximity from equilibrium state can also be seen on the enstrophy representation (Figure 2) where it can be seen that the system reaches in the first day a value of the same order of magnitude as in the day 31. An energy gap between the two initialization methods keeps up until the end of the simulation (31 December). The energy loss on the Slow Start initialization is due possibly to the density gradient diffusion during the adjustment of the velocity field to the mass field.

Looking for the time series of the kinetic energy during the run period (1 year simulation), represented on Figure 3, we can observe an annual cycle that probably is related with the annual cycle of the wind field (also in Figure 3, for the same period). In both energy and wind speed results we have filtered out the tide cycle (making a lunar period average), keeping only the low- frequency part of those quantities. [22] have compared the mean wind stress with the eddy kinetic energy climatology obtained from twelve years of sea level anomaly from altimetry data, and the two data sets shows a strong correlation. The kinetic energy obtained with the simulation that was the geostrophic initialization is very similar to those described in [22]. A lag of 2-3 months observed on the energy variability (relatively to the results of those authors) could be explained by the same difference between our wind speed variability and the mean win stress variability given in [22].

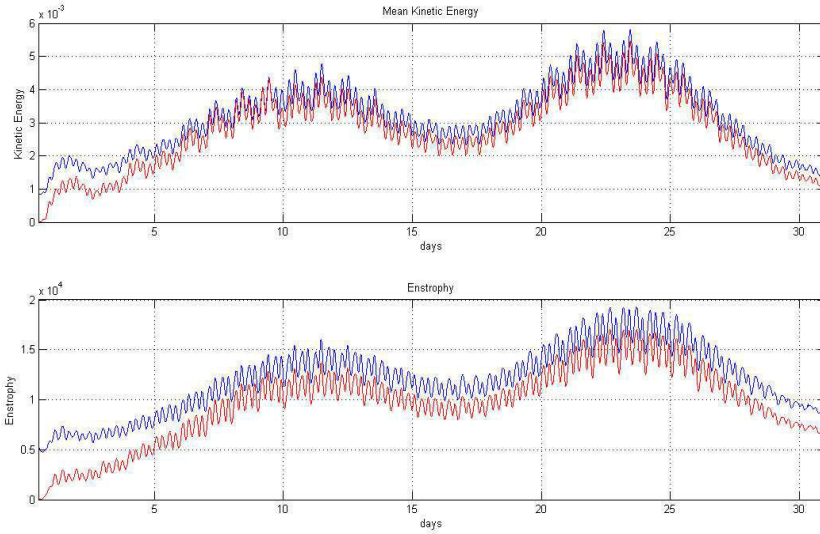


**Figure 2.** Mean relative kinetic energy ( $\text{m}^2 \text{s}^{-2}$ ) (top) and Enstrophy ( $\text{m}^2 \text{s}^{-2}$ ) variation along time (days) for the first month (bottom): Geostrophic initialization (blue line) and Slow Start initialization (red line).

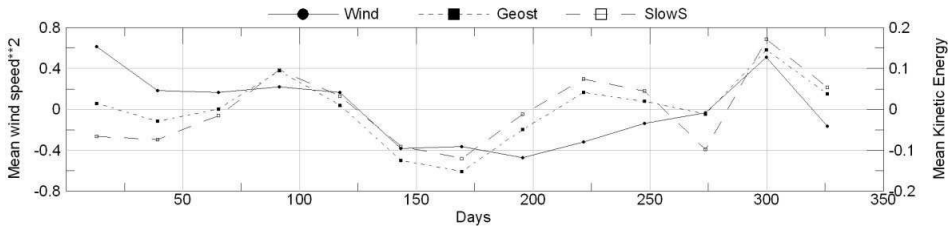


**Figure 3.** Mean relative kinetic energy and mean wind speed variation along time (days), from the filtered time series (variables are dimensionless and they represent a mean relative deviation).

The relation between those two quantities (kinetic energy and wind speed) in the Bay of Biscay is not clear on the literature. In a resume of the main aspects of the circulation on this region, [23] have estimated the current strength associated with each process. As [24] pointed out, the most energetic motion in the Bay of Biscay is connected with the high-frequency tides and internal waves. However, our time series do not consider this high-frequency kinetic energy. [24] for the Armorican shelf, in autumn, found a link between the fluctuations observed in the velocity field and wind events.

Using the filtered series of the kinetic energy and the square value of the wind speed (the wind stress is proportional to the square value of the wind speed) we have computed the Pearson correlation coefficient between those two quantities. The results are very different for each initialization scheme: 0.62 for the geostrophic initialization and 0.29 for the slow start. Taking the square of those values, we can say that: in the simulation with geostrophic velocities

initialization, 39% of the kinetic energy variability is explain by the wind speed variability; in the simulation with Slow Start initialization we have just 9% of the kinetic energy variability explained by wind speed variability.

[26] did an exhaustive study of the wind driven response: they point out the determinant role of the wind stress on the general circulation in the Bay of Biscay. Those results leads us to conclude that the model with geostrophic velocities initialization have a better wind driven response than the model with a slow start initialization. In fact, the geostrophic velocities computed with the initial density and sea level fields derived from Mercator solution give us a good approximation to a state that is dynamically in balance with the wind forcing on the entire water column. Thus, the model initialized with geostrophic velocities to have a better response to wind driven forcing than when he is initialized from the rest. To reinforce this idea we have computed for both simulations, the skewness of the difference between kinetic energy and wind speed (for both series we use the mean deviation normalized of the filtered time series). The skewness standard error is 0.62 for both distributions indicating a good symmetry relatively to the wind speed in both simulations. The results of the skewness (-0.13) to geostrophic initialization and -0.29 to slow start) shows a better fit between the kinetic energy and the wind speed for the simulation with geostrophic velocities initialization.

### 3.2 Residual Circulation

One of the main goals of the initialization with geostrophic velocities is the circulation pattern after 1 day run (Figure 4). In fact, if we compare the residual velocity field obtained after 1 day, with the results show on Figure 1, it is clear that the first one is very close to the initial solution. Particularly, the current at the Armorican slope has a very clear signature in the first 500 m with current intensities ranging between 5-10  $\text{cm s}^{-1}$  consistent with the literature.

[27] point out that those slope currents are persistent (with a seasonal variability) and its signature extends from the surface until 3-4 km depth (2-10  $\text{cm s}^{-1}$ ). An analysis of the slope current system in the Bay of Biscay show that complete flow reversals can occur if the effect of the large-scale density structure drives a weak slope current and at the same time wind blows with a strong opposite alongshore component [28-29]. Even with some undesirable transient processes over the slope during the initialization process, the solution after one month keeps the structure of the slope current. The general pattern at the first day is close to the general circulation described by [23]. The persistence of the main currents is due to the proximity of the initial state to the dynamic state of the reference solution. The balance between the mass (density and sea level) and the velocity fields gives an important stability to the model.

### 3.3 Hydrology

To analyse the Sea Surface Temperature (SST) and the vertical thermohaline structure, Microwave SST (see section 2.3 for the details) and the Argo floats profile (section 2.3) were used. Quantitative model skill metrics such as the correlation coefficient (R), the bias, the root mean square error (rmse) and the skewness of the difference between the model results and the *in situ* data was calculated. This statistics were applied to both initializations methods for one year.

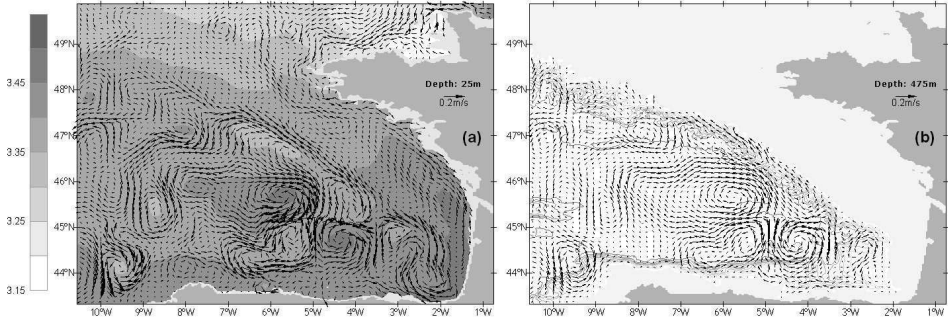


**Figure 4.** : (a) Mean Sea Surface level and residual velocities at 25 m deep after 1 days of run (2 January); (b) Bathymetry (contour interval is 500 m) and residual velocities at 475 m deep for the same period.

The results for the SST analyses (Figure 5 and Figure 6) show that both simulations have a good agreement with the data. There are not significantly differences between the initializations. Analysing the images between May and July some discrepancies can be observed at southwest boundary. Differences are due to the over-heating obtained in Mercator solution for this period, reflected in a large bias (Figure 5). Simulation with slow start initialization is more sensible to this over-heating. Initial dynamic coherence of the simulation with geostrophic velocities initialization gives to the model the ability to resist to an artificial density gradient imposed at the boundary by the reference solution.

Good “behavior” at the surface temperature leads to conclude that both simulations reach a stable solution during the initialization despite some initial inconsistencies due to crude interpolation/extrapolation of the reference solution. Figure 6 give an example of the agreement between model (with geostrophic velocities initialization) and microwave SST satellite data. The good fit between both values is clear, and statistical parameters show a small deviation between them.

Vertical thermohaline structure was analyzed with the available *in situ* data give from Argo floats. Temperature and salinity profiles and also (T,S) diagrams was compared with the data. Global results for BIAS, RMSE, Pearson correlation coefficient and skewness (Table 1) have values very close and a global analysis shows that no significant differences between the two methodologies arises (skewness was computed for the series obtained with the difference between model results and data). However, the values of skewness parameter reflect that the simulation with geostrophic velocities is more consistent with data.

Notice that the lack of Mediterranean water in Mercator solution (Figure 7) avoids a good analysis of salinity results. The best statistical results were obtained for (T,S) diagrams (density results) showing that the simulation with geostrophic velocities initialization provides a better fit with data than the slow start initialization (the skewness is improved on 3%). In both simulations the correlation coefficient and the skewness results are very satisfactory. The skewness standard error is 0.28 for both distributions.

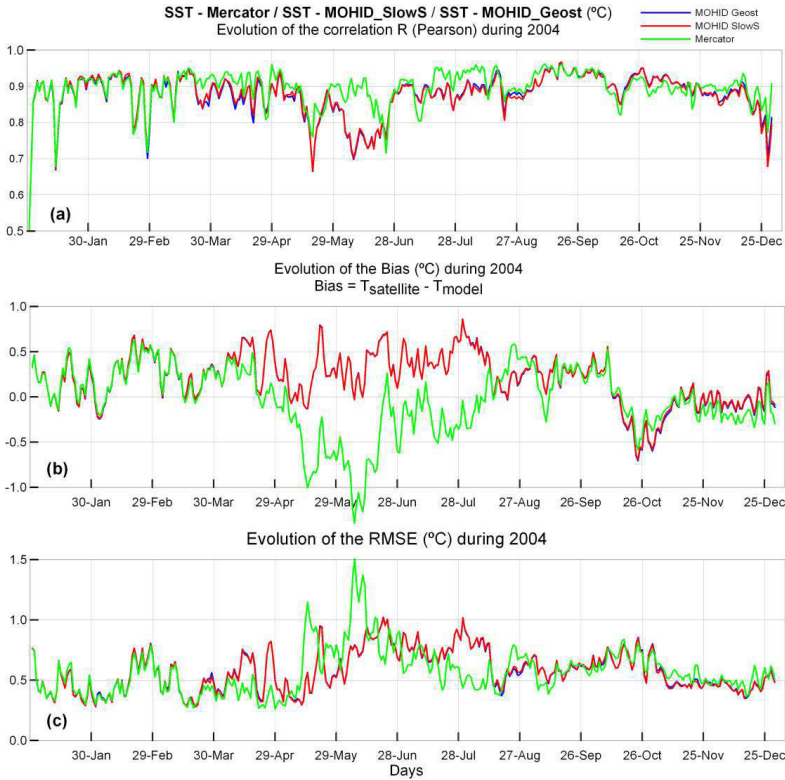


**Figure 5.** One year comparison between Microwave SST and the results of the two simulations (also for Mercator solution): (a) Pearson correlation coefficient; (b) Bias; (c) Root mean square error.

Better skewness results obtained with geostrophic initialization can be explained with the good fit on deep waters (below the Mediterranean water) that can be observed in almost (T,S) diagrams (Figure 7). The agreement of the solution with geostrophic initialization stresses the good approach of geostrophic velocities on deep waters region. Argo floats do not have the Labrador Sea Water (LSW) core but they represent quit well the transient region between Mediterranean waters and LSW. In the Bay of Biscay, the depth associated with those waters is located between 1500 m and 2000 m 88 [30]. Those water masses were detected in this area on 1993 with a core centered at 1700 dbar [31].

In order to get a relevant statistical analysis, results on different layers of 500 meters were compared. The salinity correlation coefficient for Mercator solution above 1500 meters takes values of the order of 0.5, showing that statistical conclusions cannot be achieved on those depths. Results for density in depths ranging between 1500-2000 meters (Table 2) shows that the simulation initialized with geostrophic velocities provide a better description of the vertical thermohaline structure relatively to the simulation with the slow start initialization.

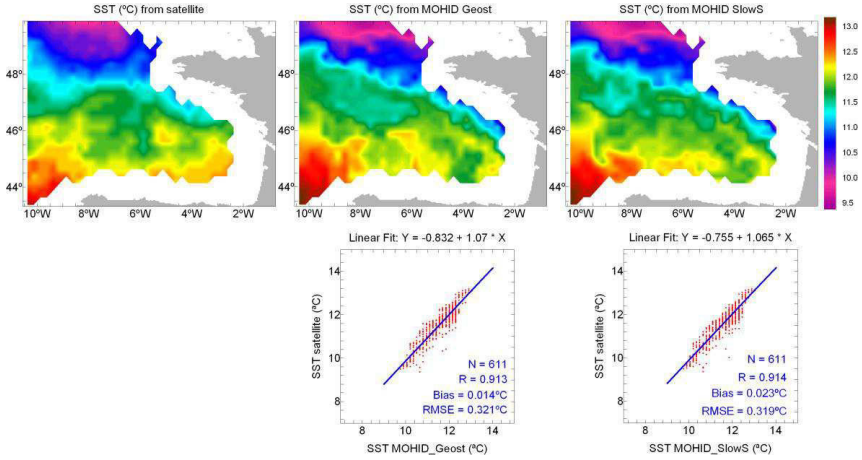


**Figure 6.** Sea Surface temperature for the day 2004-03-15 from satellite, from model initialized with geostrophic velocities and slow start methodology.

**Table 1.** Annual statistical parameters computed for simulations and Mercator solution on Argo buoys.

	Pearson correlation	Bias	RMSE	Skewness
<b>Salinity</b>				
Mercator solution	0.81	-0.078	0.15	-1.29
Geostrophic initialization	0.84	-0.077	0.14	-1.11
Slow start initialization	0.85	-0.076	0.14	-1.18
<b>Temperature</b>				
Mercator solution	0.98	-0.49	0.89	-0.31
Geostrophic initialization	0.98	-0.36	0.81	-0.66
Slow start initialization	0.98	-0.34	0.78	-0.75
<b>Density</b>				
Mercator solution	0.99	0.016	0.084	-0.85
Geostrophic initialization	0.99	-0.001	0.069	-0.38
Slow start initialization	0.99	-0.004	0.065	-0.39

**Table 2.** Annual statistical parameters computed for simulations and Mercator solution on Argo buoys (results for density in a depth ranging between 1500-2000 meters).

	Pearson correlation	Bias	RMSE
Mercator solution	0.839	0.027	0.028
Geostrophic initialization	0.847	0.001	0.016
Slow start initialization	0.826	0.000	0.019

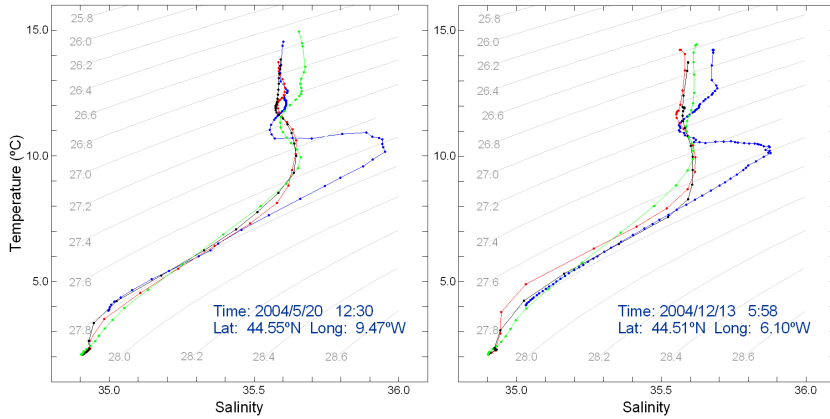


**Figure 7.** (T,S) diagrams from: Argo floats (blue line); Mercator solution (green line); simulation with geostrophic initialization (black line); simulation with slow start initialization (red line). Sigma density isolines are represented (grey lines).

#### 4 CONCLUSIONS

In a downscaling methodology, the initialization with geostrophic velocities computed from the reference solution lead the model to a stable behaviour during the spin up period. The model starts from a dynamic state allowing an instantaneous switch on of all the forcing terms associated with the reference solution. The comparison between model results and *in situ* data is very satisfactory suggesting that unrealistic transient processes associated with a crude interpolation/extrapolation do not have irreversible consequences on the model behaviour.

Comparing this alternative methodology with slow start initialization described in this paper, results show that the initialization with the geostrophic velocities avoids a decrease of kinetic energy and enstrophy during the spin up period. This difference is maintained during 1 year of simulation suggesting that the initial state of the model obtain with this method is nearest the true state.

Using the geostrophic velocities initialization, a significant correlation between total low-frequency kinetic energy and the wind speed was observed for the Bay of Biscay. This correlation seems to be compatible with the literature, and seem to be an advantage relatively to the initialization with slow start method.

This methodology is particularly important in deep zones leading to a good thermo-haline description of the deep waters. Results show that, on deep zones geostrophic velocity initialization improves the solution obtained with slow start methodology. The (T,S) diagrams indicates an hydrologic structure compatible with literature.

This affordable initialization approach has a very low computational cost relatively to variational methods, and leads the model to a near true initial state. Relatively to the slow start initialization, the spin up time is drastically reduced. Those arguments could be an advantage to use this methodology on operational Oceanography.

## ACKNOWLEDGEMENTS

This work was carried out in the frame of INSEA program. The authors wish to thank Ramiro Neves, Guillaume Rifflet, Rodrigo Fernandes and Nuno Vaz for their contributions during this work. A special thanks to Ricardo Lemos for helping us with statistical analysis.

## REFERENCES

1. Leitão P., H. Coelho, A. Santos, R. Neves 2005. Modelling the main features of the algarve coastal circulation during july 2004: A downscaling approach. *Journal of Atmospheric & Ocean Science*. 10 (4): 421-462.
2. Auclair F., P. Marsaleix and C. Estournel, 2001. The penetration of the Northern Current over the Gulf of Lions (Mediterranean) as a downscaling problem. *Oceanologica Acta*. 24: 529–544.
3. Malanotte-Rizzoli P., R. E. Young, and D. B. Haidvogel, 1989: Initialization and data assimilation experiments with a primitive equation model. *Dynamics of Atmospheres and Oceans*. 13, 349–378.
4. Auclair F., S. Casitas and P. Marsaleix 2000. Application of an Inverse Method to Coastal Modeling. *Journal of atmospheric and oceanic technology*. 17: 1368-1391.
5. Woodgate R. A., and P. D. Killworth, 1997: The effects of assimilation on the physics of an ocean model. Part I: Theoretical model and barotropic results. *Journal of atmospheric and oceanic technology*. 14: 897–909.
6. Woodgate R. A., 1997: The effects of assimilation on the physics of an ocean model. Part II: Baroclinic identical-twin experiments. *Journal of atmospheric and oceanic technology*. 14: 910–924.
7. Marchesiello P., J. C. McWilliams and A. Shchepetkin 2001. Open boundary conditions for long-term integration of regional oceanic models. *Ocean Modelling* 3, 1-20.
8. Martinsen E.A., and H. Engedahl. 1987. Implementation and testing of a lateral boundary scheme as an open boundary condition in a barotropic ocean model. *Coastal Engineering*. 11, 603-627.
9. Flather R.A. 1976. A tidal model of the northwest European continental shelf. *Memoires Societe Royale des Science de Liege*. 6 (10), 141-164.
10. Coelho H., R. Neves, M. White, P. Leitão and A. Santos 2002. A model for ocean circulation on the Iberian coast. *Journal of Marine Systems*. 33: 153-179.
11. Gunson J. R. and P. Malanotte-Rizolli 1996. Assimilation studies of open-ocean flows .1. Estimation of initial and boundary conditions. *Journal of Geophysical Research*. 101, C12, 28457-28472.
12. De Mey, P., 1997: Data assimilation at the oceanic mesoscale: A review. *Journal of the Meteorological Society of Japan*. 75: 415–427.
13. Estournel C., X. Durrieu de Madron, P. Marsaleix, F. Auclair, C. Julliard and R. Vehil 2003. Observation and modeling of the winter coastal oceanic circulation in the gulf of Lion under wind influenced by the continental orography (FETCH experiment). *Journal of Geophysical Research*. 108, C3, 8059, doi:10.1029/2001JC000825.
14. Auclair F., C. Estournel, P. Marsaleix and I. Pairaud 2006. On Coastal ocean embedded modelling. *Geophysical Research Letters*. 33, L14602, poi:10.1029/2006GL026099.
15. Estournel C., F. Auclair, M. Lux, C. Nguyen and P. Marsaleix 2007. “Scale oriented” embedded modeling of the North-Western Mediterranean in the frame of MFSTEP. *Ocean Science Discussions*. 4: 145-187.
16. Vaz N., L. Fernandes, P.C. Leitão, J.M. Dias, R.Neves (this issue). The Tagus estuarine plume forced by freshwater inflow and wind.
17. Chippada S., C. Dawson, M. Wheeler, 1998. A Godonov-type finite volume method for the system of shallow water equations. *Computer Methods in Applied Mechanics and Engineering*. 151(01): 105-130.
18. Martins F., R. Neves, P.C. Leitão, and A. Silva (2001) 3D modeling in the Sado estuary using a new generic coordinate approach. *Oceanologica Acta*. 24, S51-S62.
19. Gould, J., and the Argo steering team, 2004: Argo profiling floats bring new era of in situ ocean observations. *Eos Trans. AGU*, 85(19), 185, doi:10.1029/2004EO190002.

20. Reynolds, R. W., N. A. Rayner, T. M. Smith, D. C. Strokes, and W. Wang, 2002: An improved in situ and satellite SST analysis for climate. *Journal of Climate*. 15, 1609-1625.
21. Vazquez-Cuervo, J., E. M. Armstrong, and A. Harris, 2004: The effect of aerosols and clouds on the retrieval of infrared sea surface temperature. *Journal of Climate*. 17: 3921-3933.
22. Caballero A., A. Pascual, G. Dibarbouré and M. Espino 2008. Sea level and Eddy Kinetic Energy variability in the Bay of Biscay, inferred from satellite altimeter data. *Journal of Marine Systems*. 72: 116-134.
23. Koutsikopoulos, C. and B. Le Cann 1996. Physical processes and hydrological structures related to the Bay of Biscay anchovy. *Scientia Marina*. 60 (Supl. 2): 9-19.
24. Van Aken H. M. 2002. Surface currents in the Bay of Biscay as observed with drifters between 1995 and 1999. *Deep-Sea Research I*. 49: 1071–1086.
25. Lazure P., F. Dumas and C. Vrignaud 2008. Circulation on the Armorican shelf (Bay of Biscay) in autumn. *Journal of Marine Systems*. 72: 218-237.
26. Pingree R. D. and B. Le Cann 1989. Celtic and Armorican slope and shelf residual currents. *Prog. Oceanog*. 23: 303-338.
27. Pingree R. D. and B. Le Cann 1990. Structure strength and seasonality of the slope currents in the Bay of Biscay region. *J. Mar biol. Ass. U.K.* 70:857-855.
28. Friocourt, Y., B. Levier, S. S. Drijfhour and B. Blanke 2008. On the Dynamics of the Slope Current System along the West European Margin. Part I: Analytical Calculations and Numerical Simulations with Steady-State Forcing. *Journal of Physical Oceanography*. 38: 2597-2618.
29. Friocourt, Y., B. Levier, S. S. Drijfhour and B. Blanke 2008. On the Dynamics of the Slope Current System along the West European Margin. Part II: Analytical Calculations and Numerical Simulations with Seasonal Forcing. *Journal of Physical Oceanography*. 38: 2619-2638.
30. Friocourt, Y., B. Levier, S. Speich, B. Blanke and S. S. Drijfhour 2007. A regional numerical ocean model of the circulation in the Bay of Biscay. *Journal of Geophysical Research*. 112, C09008, doi:10.1029/2006JCC003935.
31. Fiuza A. F. G., M. Hamann, I. Âmbar, G. Diaz del Rio, N. González and J. M. Cabanas 1998. Water Masses and their circulation off western Ibéria during May 1993. *Deep-Sea Research I*. 45: 1127-1160.